3D Fiber-Based Hybrid Nanogenerator for Energy Harvesting and as a Self-Powered Pressure Sensor

Xiuhan Li,[†,‡,∥] Zong-Hong Lin,[†,§,∥] Gang Cheng,[†] Xiaonan Wen,[†] Ying Liu,[†] Simiao Niu,[†] and Zhong Lin Wang*[,†,⊥]

[†]School of Materials Science and Engineering, Georgia Institute of Technology, Atlanta, Georgia 30332, United States, [‡]School of Electronic and Information Engineering, Beijing Jiaotong University, Beijing 100044, China, [§]Institute of Biomedical Engineering, National Tsing Hua University, Hsinchu 30013, Taiwan, and [⊥]Beijing Institute of Nanoenergy and Nanosystems, Chinese Academy of Sciences, Beijing 100083, China. [∥]These authors contributed equally to this work.

ABSTRACT In the past years, scientists have shown that development of a power suit is no longer a dream by integrating the piezoelectric nanogenerator (PENG) or triboelectric nanogenerator (TENG) with commercial carbon fiber cloth. However, there is still no design applying those two kinds of NG together to collect the mechanical energy more efficiently. In this paper, we demonstrate a fiber-based hybrid nanogenerator (FBHNG) composed of TENG and PENG to collect the mechanical energy in the environment. The FBHNG is three-dimensional and can harvest the energy from all directions. The TENG is positioned in the core and covered with PENG as a coaxial core/shell structure. The PENG design here not only enhances the collection efficiency of mechanical energy by a single carbon fiber but also generates electric output when the TENG is not working. We also show the potential that the FBHNG can be weaved into a smart cloth to harvest the mechanical energy from human motions and act as a self-powered strain sensor. The instantaneous output power density of TENG and PENG can achieve 42.6 and 10.2 mW/m^2, respectively. And the rectified output of FBHNG has been applied to charge the commercial capacitor and drive light-emitting diodes, which are also designed as a self-powered alert system.

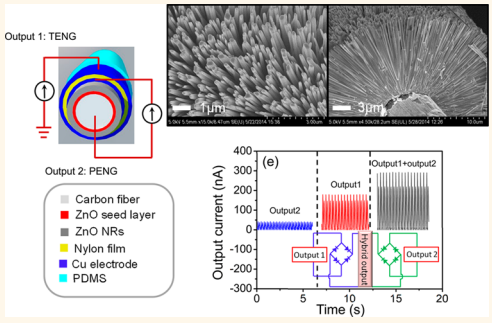

KEYWORDS: energy harvesting · triboelectric nanogenerator · piezoelectric nanogenerator · hybrid · fiber · flexible

Energy harvesting from our living environment to power portable electronic devices and sensors is a kind of green energy and have attracted worldwide attention.[1−4] Mechanical energy is a huge resource in our daily life with various energy scales and types such as wind energy to mechanical vibration,[5] flowing air and water,[6,7] human motion,[8] and muscle stretching.[9] Smart clothes composed of functional fibers integrated with nanostructures can be used for the purpose of generating power by harvesting mechanical energy and self-powered sensors.[6,10−12] It has great potential in building self-powered human motion-detecting,[13] health-monitoring, [14] and antitheft systems.[15]

Scientists have tried to put forward the concept of power and smart suit.[16] Both the piezoelectric and triboelectric nanostructures (PENG and TENG) have been integrated onto the fibers and convert the mechanical energy into electricity.[6,12] Recently, hybrid nanogenerators (NGs) combining two power generation mechanisms have attracted more attention.[17] TENG hybrid with PENG,[18] TENG hybrid with electromagnetic induction generator,[19] and TENG hybrid with flowing water[20] have been studied to improve power generate efficiency. The critical design issue for hybrid NG is the integrated fabrication method and how to combine different energy harvest mechanism. To design a fully integrated fiber-based hybrid nanogenerator (FBHNG) composed of TENG and PENG, we need to understand the working mechanism of TENG and PENG first. The basic working principle for TENG is a combination of contact electrification and electrostatic induction. The successive current is gained through the charge transfer from the multiple in-plane charge separation cycles.[21,22] There is no output for TENG without contact and separate motion. Although the TENGs have high energy collection efficiency which is much larger than

* Address correspondence to zlwang@gatech.edu.

Received for review July 31, 2014 and accepted September 26, 2014.

Published online 10.1021/nn504243j

PENG, the piezoelectric polarization charges of the PENG can be created at the end of each nanostructure by applying strain, pressure or force.[23−26] Therefore, the PENG have excellent sensitivity to external strain, which is an advantage over TENG. In addition, the PENG can be a supplement for TENG. The PENG studied here not only improve the power convert efficiency of FBHNG but also provide output under the circumstance without contact and separate motion.

For FBHNG, the structure design and fabrication method is the key issue. To enhance the conversion efficiency and the excellent adaptability of the FBHNG, the fabrication of ZnO nanorods (NRs) on fibers has an important role. Coaxial functional fiber can be verified through 3D fabrication method on the carbon fibers. Due to its lightweight, inexpensive, conductive and foldable character, carbon fibers were demonstrated to be an efficient substrate for FBHNG.[6,12] The ZnO NRs have been successfully grown on the carbon fibers by physical evaporation deposition (PVD)[6] and hydrothermal growth approach.[24] The length of ZnO NRs can be further increased by adding ammonia into the reaction solution.[25] And the prepared longer ZnO NRs have been demonstrated to have larger piezo-potential. In those studies, ZnO NRs were grown radially around the carbon fibers, thus designing an all-round electrode which could utilize all ZnO NRs on fiber is an effective way to increase the contact area and improve the energy output. The flexible polymer film could be folded in any angle and is a perfect candidate of all-round electrode both for PENG and TENG. Construction of FBHNG using the foldable polymer film with sputtered copper electrode on both sides is a feasible way to enhance the output of FBHNG. In addition, triboelectric nanomaterials such as PVDF (polyvinylidene fluoride) has also been integrated on the carbon fibers and the corresponding TENG have been developed.[12]

In this paper, we design a fully integrated TENG and PENG on the carbon fiber cloth which contains numerous carbon fibers as shown in Supporting Information Figure S1a. The FBHNG is very flexible and can be utilized to fabricate smart cloth for the purpose of collecting the mechanical/kinetic energy from ambient environment. We demonstrate a novel, low-cost 3D fabrication method to fabricate FBHNG consisting of central ZnO NRs on carbon fibers and outer foldable double side cooper coated nylon film as tribo- and piezo-electrode. Coaxial functional fiber with PENG inside and TENG outside were fully integrated on a carbon fiber cloth. PENG is the supplement for TENG which can also generate power and act as strain sensor under the motion mode without TENG. 3D coaxial structure ensured that the TENG and PENG have the same action axis and can improve the effective impact area greatly. ZnO NRs with the length of 10 μm were successfully grown around the conductive carbon fibers by hydrothermal growth approach. The output current and voltage of the TENG and the PENG were characterized by a mechanical motor. The measured instantaneous power density of 12 contact array points for TENG and PENG is 42.6 and 10.2 mW/m^2, respectively. The instantaneous power density and current density for FBHNG could multiply with the increasing of contact array points and area. The rectified outputs have been applied to charge commercial capacitors and drive light-emitting diodes which can be stored in a capacitor and used in a self-powered alert system. in addition, the FBHNG can be used as a self-powered sensor to detect human elbow motion.

RESULTS AND DISCUSSION

The fabrication process of the FBHNG is schematically depicted in Figure 1a. Basically, the FBHNG is a 3D coaxial and fully integrated device containing a PENG unit (Output 2) in the core and a TENG unit (Output 1) in the shell. Before the fabrication process, the carbon fiber cloth was cleaned sequentially with acetone, ethanol, and deionized water. First, a 250 nm ZnO thin film was sputtered on the carbon fiber as the seed layer (i). Then, the ZnO NRs were grown on the ZnO seed layer through the hydrothermal method (ii).[24] Typically, the growth solution contained equal volume (50 mM) of zinc nitrate hexahydrate, hexamethylenetetramine (HMTA) (50 mM) and ammonia−water (7 mM) in deionized water and the reaction temperature was fixed at 85 °C for 12 h. As shown in SEM image (Figure1b−d), ZnO NRs are uniformly distributed on each fiber and the length of the ZnO NRs is 10 μm. In the other way, metal thin films of Ti/Cu (100 nm) were sputtered on both sides of a nylon film as the conducting electrodes (iii). The inner Ti/Cu thin film acted as the top electrode of PENG and the outer Ti/Cu thin film was the output electrode (Output 1) of TENG. The Ti/Cu-coated nylon film was wrapped around the carbon fiber and packaged in a tube mold with a diameter of 3 mm by polydimethylsiloxane (PDMS) (iv). The elastomer and the cross-linker of PDMS were mixed in a 10:1 weight ratio. After the mixture was degassed for 2 h, the carbon fibers and the Ti/Cu-coated nylon film were immersed in the mixture and degassed again to fully fill the tube. After the solution was further heated at 85 °C for 1 h, the coaxial FBHNG with TENG outside and PENG inside was obtained. Before the test of the prepared FBHNG, the mold needs to be peeled. The SEM image of the cross section of FBHNG was shown in Supporting Information Figure S1b.

The working mechanisms of the FBHNG can be explained separately as a TENG and a PENG, which is shown in Figure 2. A clear cross section of the FBHNG is shown in Figure 2a. For optimization of the output of the TENG, we choose the nylon fiber as the other contact material to deform the FBHNG. When the nylon fiber contacts the PDMS layer, the electrons on the nylon fiber surface will transfer to the PDMS layer and

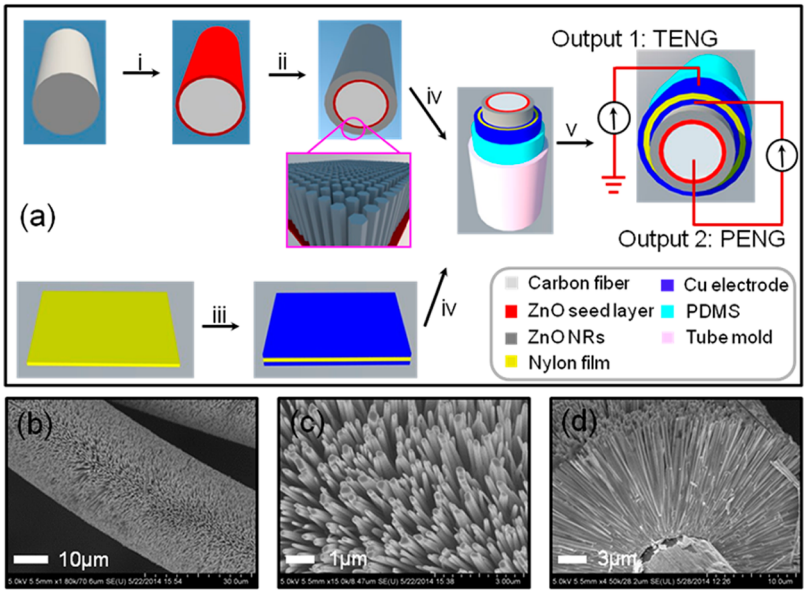

Figure 1. Fully integrated 3D fabrication method for FBHNG. (a) Fabrication process step for 3D Coaxial FBHNG. (i) Depositing of ZnO seed layer by PVD; (ii) growing of ZnO NRs around carbon fiber by hydrothermal method; (iii) depositing of double side copper electrode on nylon film; (iv) assembling the carbon fibers and nylon film into tube mold by PDMS; (v) peeling of FBHNG from the tube mold. SEM images for the whole fiber with ZnO NRs (b), top view of ZnO NRs (c), and cross-sectional view of ZnO NRs (d).

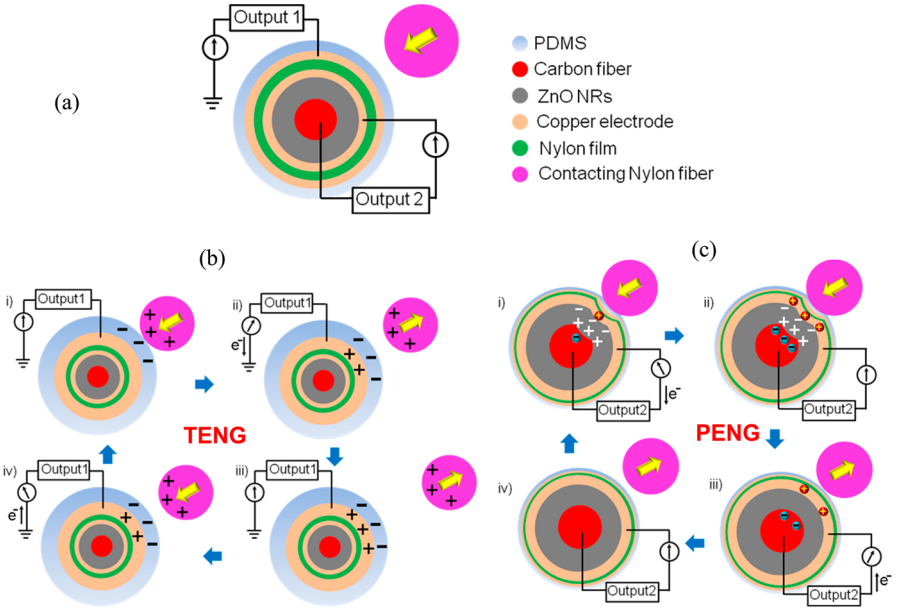

Figure 2. Working mechanism for 3D coaxial FBHNG. (a) Certain area of the cross section is schematically shown. (b) Working mechanism of TENG when the functional fiber contact and separate with another fiber. (c) Illustrated working mechanism of PENG when the functional fiber press and release from another fiber.

create charged surfaces of the PDMS layer and the nylon fiber (i). Once the nylon fiber leaves, a negative electric potential difference between the PDMS layer and the ground is established (ii). The electrons will flow from the outer Cu electrode to the ground through the external load and finally reach equilibrium (iii). This contributes to the positive pulse output current of TENG from Output 1. As the nylon fiber approaches the PDMS layer, a positive electric potential difference between the PDMS layer and the ground is formed. This will cause the electrons flow from the outer Cu electrode to the ground and contribute to the negative pulse output current of TENG from Output 1 (iv), until achieving another equilibrium (i). At the same time, when the FBHNG is deformed by the nylon fiber, the inner PENG also starts to work because of the coaxial structure. The ZnO NRs on the carbon fiber are compressively strained and a positive electric potential difference is formed between the inner Cu electrode and the conductive carbon fiber (i).[25−30] This will force

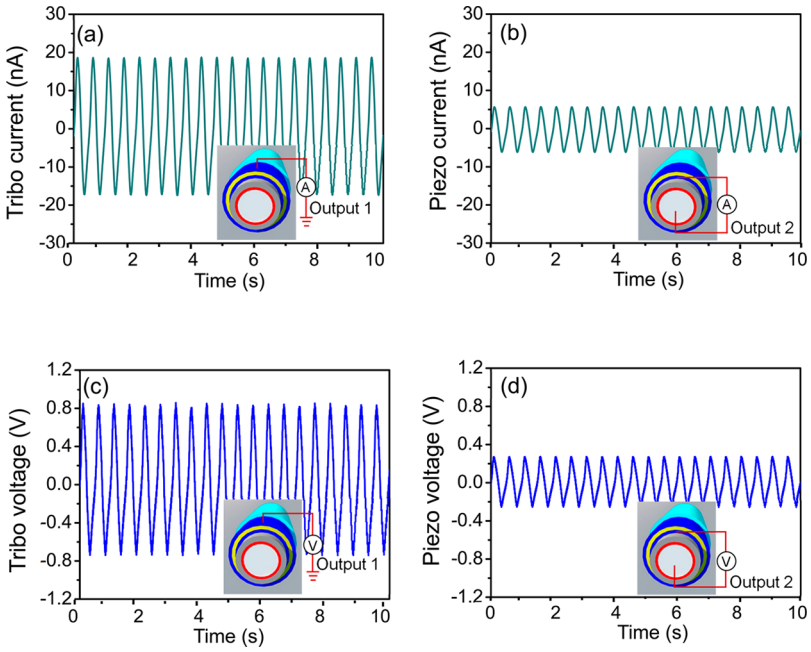

Figure 3. Measurement results for one FBHNG contact with one nylon fiber driven by Shaker motor (contact area is 9 mm^2). (a and c) Current and voltage generated by TENG; (b and d) Current and voltage generated by PENG.

the electrons to flow from the inner Cu electrode to the carbon fiber through the external load and contribute to the positive pulse output current of PENG from Output 2, until reaching equilibrium (ii). As the nylon fiber leaves and the compressive strain is released, the piezoelectric potential will be diminished. The electrons accumulated at the carbon fiber will flow back to the inner Cu electrode, generating the negative pulse output current of PENG from Output 2 (iii), finally reaching another equilibrium (iv). The continuous output of the FBHNG from Output 1 (TENG) and Output 2 (PENG) can be provided once the nylon fiber repeatedly deforms and separates from the FBHNG.

To demonstrate the working mode of the FBHNG, a mechanical motor is used as the applied force to ensure the contact of fibers. The nylon fiber is attached on the motor and will periodically contact and separate from the FBHNG. The short-circuit current (I_{sc}) and open-circuit voltage (V_{oc}) were measured to characterize the performance of the FBHNG. Figure 3 shows the outputs from Output 1 and Output 2. The effective contact area between the FBHNG and the nylon fiber is assumed to be 9 mm^2. Upon the impacting frequency of 2 Hz, the generated current from Output 1 is 20 nA (Figure 3a) and the generated current for Output 2 is 5.5 nA (Figure 3b). The generated voltage from Output 1 can reach 1.5 V (Figure 3c), while the generated voltage from Output 2 has a lower value of 0.5 V (Figure 3d). We can observe that the generated output from TENG (Output 1) is higher than that from PENG (Output 2).

The main advantage of the FBHNG is that it can be easy to increase the number of working unit, which will consequently increase the contact area and generated output. The electrical connection of multiple FBHNG is illustrated in Figure 4a,b. TENGs are connected in parallel through the outer Cu electrodes in each FBHNG unit, while the other ends of each TENG are connected to the ground. PENGs are also connected in parallel through the conductive carbon fibers and the inner Cu electrode on the bottom side of the nylon film. The simulation results of the electrostatic field distribution for one FBHNG contact with multiple nylon fibers by Comsol Multiphysics were given in Supporting Information Figure S2. The computed electrostatic field around the fibers and the corresponding charge transfer (ΔQ)indicated that the field strength was increasing with the number of contact fibers. The relationship between the output current and different number of contact fibers was compared in Figure 4c (the area for different number of contact fibers is 9, 27, 54, 81, and 108 mm^2). The output current from both Output 1 and Output 2 were increased with the contact area. The output current from Output 1 varied from 20 to180 nA as the contact area is increased from 9 to 108 mm^2. We observed that the output current from Output 1 is much higher than that from Output 2. The measured ΔQ for FBHNG is also proportional to the contact area, which is similar to the simulation results (Figure 4d). The rectified output currents from Output 1 and Output 2 were measured and shown in Figure 4e. To present that the generated output of FBHNG can be effectively utilized to charge the capacitor or battery, the rectified output currents from Output 1 and Output 2 were connected in parallel. The results clearly indicate that the total rectified output current is equal

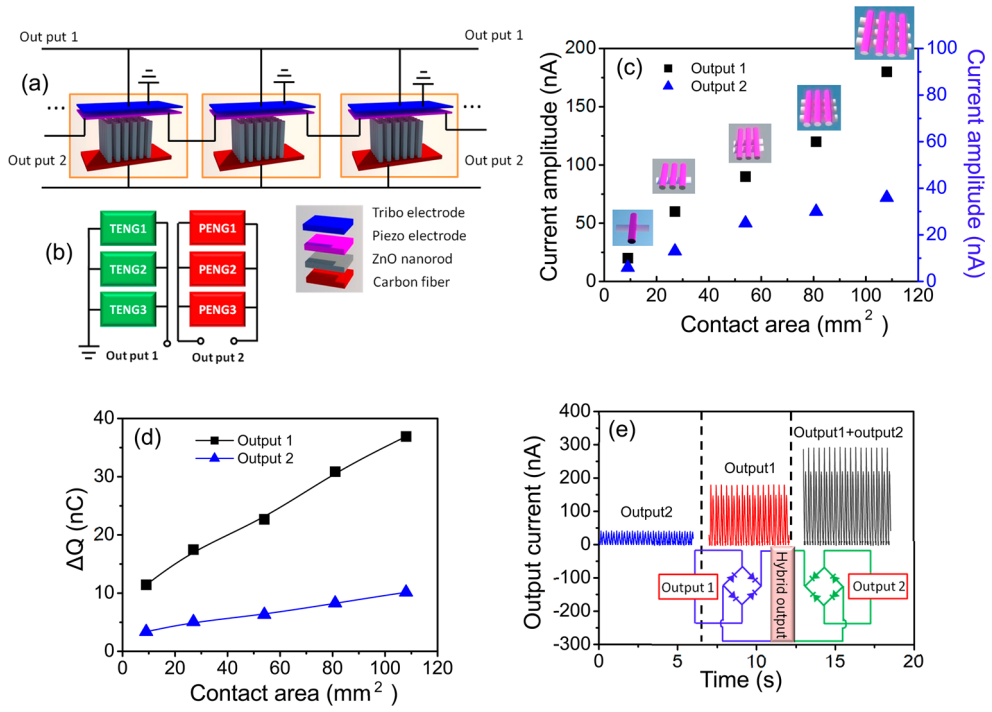

Figure 4. (a) Schematic of physical connection for TENG and PENG. (b) The circuit topology for three TENGs and PENGs. (c) Measured output current when varying the contact area. (d) Total charge transfer of FBHNG when varying the contact area. (e) The rectified output current for Output 1, Output 2 and FBHNG (Output 1 + Output 2), the contact point for FBHNG is 12 (the effective area is 108 mm^2).

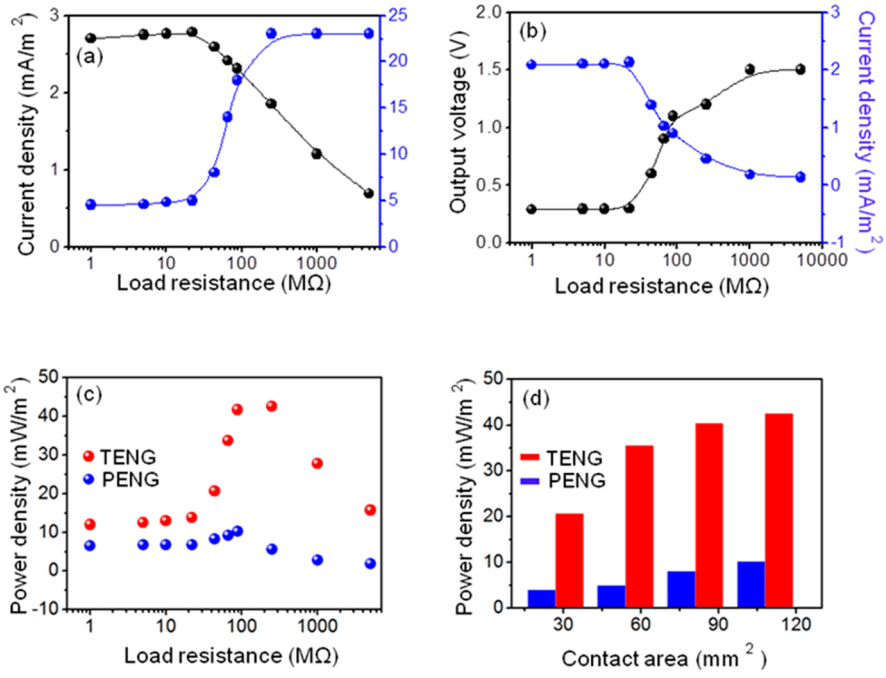

Figure 5. Output current density and voltage of TENG (a) and PENG (b) when changing the load resistance. (c) Output power density of TENG and PENG when changing the load resistance. (d) Instantaneous power density increased with the contact area for TENG and PENG under the load resistance of 88MΩ.

to the separate rectified output current from Output 1 and Output 2.

To characterize the maximum output power density of the FBHNG, different load resistances were connected to the Output 1 and Output 2 at a working frequency of 2 Hz. The load resistances were varied from 5 MΩ to 5 GΩ. As the results displayed in Figure 5a and b, when the resistance was below 10 MΩ, the generated voltages from Output 1 and Output 2 of FBHNG were close to 0 and the generated currents

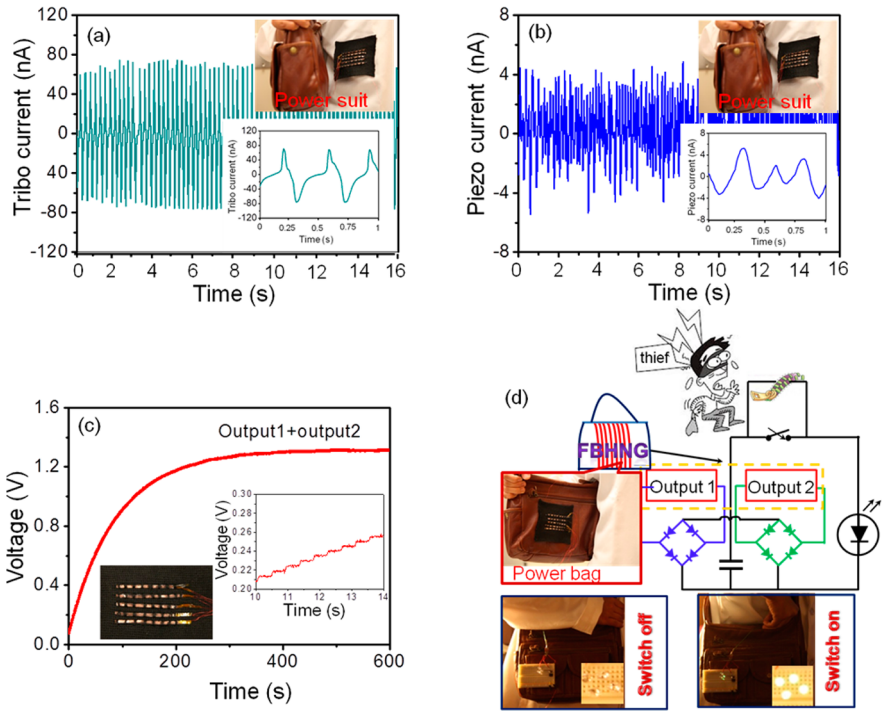

Figure 6. Generated current from Output 1 (a) and Output 2 (b) of power suit with FBHNG weaved in under the impact of human motion. (c) Charging curves of 2.2 μF capacitors by the rectified outputs from Output 1 and Output 2 of hybrid NGs. (d) The photograph of the rectified outputs from Output 1 and Output 2 to charge a capacitor and being used in bag burglar proof system.

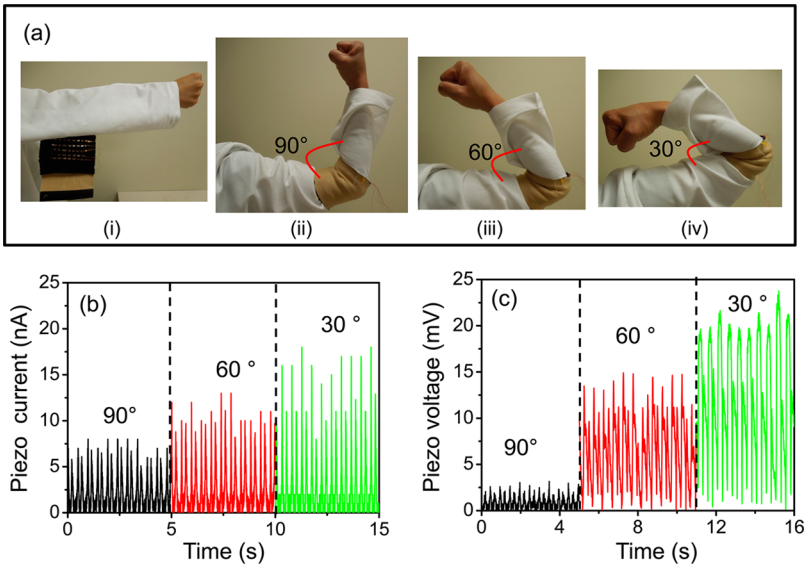

Figure 7. Weaved FBHNG detect the bending angle of arms. (a) Schematic of weaved fiber NGs impact with the arms. (b) The output current of PENGs under different bending angle. (c) The output voltage of PENGs under different bending angle.

from Output 1 and Output 2 have only slight changes. As the load resistance increased from 10 MΩ to 2 GΩ, the generated voltage from Output 1 and Output 2 through the load resistance was generally increase. Meanwhile, the generated current from Output 1 and Output 2 of FBHNG across the load resistance decreased. Dependence of instantaneous power density from Output 1 and Output 2 of FBHNG on the resistance of the external load was shown in Figure 5c. The maximum values of instantaneous power density for Output 1 and Output 2 are 42.6 mW/m^2 (250 MΩ) and 10.2 mW/m^2 (88 MΩ), respectively. The relationship between the instantaneous power density and contact area was compared in Figure 5d at a load resistance of 88 MΩ. It is clearly indicated that the instantaneous power density was also increased with the contact area of both TENG and PENG.

To address the potential applications of the FBHNG, we demonstrate the FBHNG can be weaved with cotton

fiber to become a power cloth or power bag. The generated current from Output 1 of 5 weaved FBHNGs can reach 70 nA (Figure 6a), while the generated current from Output 2 of 5 weaved FBHNGs is 4 nA (Figure 6b). The generated outputs then connect to a full-wave rectifying bridge to transform the AC outputs to a same direction and charge a 2.2 μF capacitor (Figure 6c). By applying commercial LEDs as an indicator, we design a self-powered alert system (Figure 6d). Once the bag is opened, the sliding of zipper changes the switch to an "on" status and the LEDs will be turned on. This can remind the owner to be careful of the bag. The FBHNG can also function as a self-powered strain sensor for monitoring health condition. As shown in Figure 7a, the weaved FBHNGs were fixed tightly on the elbow. When the elbow bends at different angles (90°, 60°, and 30°), the generated outputs from the PENG of the weaved FBHNGs are different (Figure 7b,c). This is because the smaller the bending angle, the larger the applied bending strain is on the ZnO NRs, therefore generating more enhanced output. The stimulation data of the piezopotential distribution along the ZnO NRs under different strains are calculated by Comsol Multiphysics (Supporting Information Figure S3). It is clearly shown that the piezo-potential along the ZnO NRs changes linearly with the strain ratio, which verifies the experimental results.

CONCLUSION

In summary, a newly designed FBHNG is developed by integrating the TENG and PENG on coaxial carbon fiber cloth. The FBHNG can be more efficient at harvesting the mechanical energy as compared to the individual TENG or PENG. The presence of PENG in the hybrid structure is a supplement for TENG which can still generate output when the TENG is not working in certain situations. The generated instantaneous power density for TENG and PENG can achieve 42.6 and 10.2 mW/m^2, respectively. We also demonstrated that the total charge transfer, output current, and instantaneous power density can be largely enhanced by increasing the area and number of FBHNG, which shows the potential in producing the power cloth and suit. The combination of commercial LEDs with FBHNG indicates that it could be used in a self-powered alert system. Besides, the FBHNG can also function as a self-powered strain sensor for monitoring health condition.

METHODS

Fabrication of ZnO NRs on Carbon Fibers. Well-aligned ZnO NR arrays were grown on the fiber using the following steps: (i) Before the growth of ZnO NWs, the carbon fibers were cleaned ultrasonically in acetone, ethanol, and deionized water. (ii) Compacted ZnO seed layer of 250 nm was sputtered on the carbon fibers by PVD75 (Kurt J. Lesker Company PRO Line PVD 75). (iii) The ZnO NRs were grown on the ZnO seed coated carbon fibers through a hydrothermal method. The growth solution contained equal volumes (50 mM) of zinc nitrate hexahydrate, hexamethylenetetramine (HMTA) (50 mM) and ammonia−water (7 mM) in deionized water and the growth took place for 12 h at 85 °C. Finally, the ZnO NRs were grown radially around the carbon fibers.

Fabrication of the FBHNG. Metal thin films of Ti/Cu (100 nm) were sputtered on both sides of a flexible nylon film as the conducting electrodes. Then, the Ti/Cu-coated nylon film was wrapped around the carbon fiber growing with ZnO NRs and packaged in a tube mold with a diameter of 3 mm by PDMS. The elastomer and the cross-linker of PDMS were mixed in a 10:1 weight ratio. After the mixture was degassed for 2 h, the carbon fibers and the Ti/Cu-coated nylon film were immersed in the mixture and degassed again to fully fill the tube. After the mixture was heated further at 85 °C for 1 h, the coaxial FBHNG with TENG outside and PENG inside was obtained. The FBHNG was finally obtained by peeling from the tube mold.

Characterization. A Hitachi SU8010 field emission scanning electron microscope (SEM) was used to measure the size and height of ZnO NRs. In the electric output measurement of the FBHNG, Shaker motor (Labworks SC121) were used to drive the FBHNG contact and separate with the nylon fibers. For the measurement of electrical outputs of TENG, a programmable electrometer (Keithley model 6514) and a low noise current preamplifier (Stanford Research System modelSR570) were used.

Conflict of Interest: The authors declare no competing financial interest.

Supporting Information Available: More detailed information about the 2D simulation results by COMSOL Multiphysics; the calculated and compared electrostatic filed two-dimensional distribution model around one FBHNG contact with one nylon fiber, two nylon fibers and three nylon fibers theoretically; the calculated two-dimensional piezo-potential distribution along singe ZnO NR (with the width of 100 nm and length of 10um) under different strain ratio (0.01%, 0.03% and 0.05%). This material is available free of charge *via* the Internet at http://pubs.acs.org.

Acknowledgment. Research was supported by Basic Energy Sciences DOE, MURI from the Airforce, the Hightower Chair Foundation, the "Thousands Talents" program for a pioneer researcher and his innovation team, Beijing National Science Foundation (4122058), Beijing Higher Education Young Elite Teacher Project (YETP0536), National Natural Science Foundation of China (60706031), and the Fundamental Research Funds for the Central Universities (2014JBM009).

REFERENCES AND NOTES

1. Wang, Z. L.; Zhu, G.; Yang, Y.; Wang, S. H.; Pan, C. F. Progress in Nanogenerators for Portable Electronics. *Mater. Today* **2012**, *15*, 532–543.
2. Wang, Z. L.; Wu, W. Nanotechnology-Enabled Energy Harvesting for Self-Powered Micro-/Nanosystems. *Angew. Chem., Int. Ed.* **2012**, *51*, 11700–11721.
3. Cheng, G.; Lin, Z.-H.; Du, Z.; Wang, Z. L. Increase Output Energy and Operation Frequency of a Triboelectric Nanogenerator by Two Grounded Electrodes Approach. *Adv. Funct. Mater.* **2014**, *24*, 2892–2898.
4. Hou, T.-C.; Yang, Y.; Zhang, H. L.; Chen, L.-J.; Chen, L. J.; Wang, Z. L. Triboelectric Nanogenerator Built inside Shoe Insole for Harvesting Walking Energy. *Nano Energy* **2013**, *2*, 856–862.
5. Hu, Y.; Yang, J.; Jing, Q. S.; Niu, S. M.; Wu, W.; Wang, Z. L. Triboelectric Nanogenerator Built on Suspended 3D Spiral Structure asVibration and Positioning Sensor and Wave Energy Harvester. *ACS Nano* **2013**, *7*, 10424–10432.
6. Li, Z.; Wang, Z. L. Air/liquid-pressure and Heartbeat-Driven Flexible Fiber Nanogenerators as a Micro/Nano-Power

Source or Diagnostic Sensor. *Adv. Mater.* **2011**, *23*, 84–89.
7. Lin, Z.-H.; Cheng, G.; Lee, S.; Pradel, C. K.; Wang, Z. L. Harvesting Water Drop Energy by a Sequential Contact-Electrification and Electrostatic-Induction Process. *Adv. Mater.* **2014**, *26*, 4690–4696.
8. Bai, P.; Zhu, G.; Lin, Z.-H.; Jing, Q. S.; Chen, J.; Zhang, G.; Ma, J.; Wang, Z. L. Integrated Multilayered Triboelectric Nanogenerator for Harvesting Biomechanical Energy from Human Motions. *ACS Nano* **2013**, *7*, 3713–3719.
9. Li, Z.; Zhu, G.; Yang, R.; Wang, A. C.; Wang, Z. L. Muscle-Driven *in Vivo* Nanogenerator. *Adv. Mater.* **2010**, *22*, 2534–2537.
10. Weng, W.; Sun, Q.; Zhang, Y.; Lin, H.; Ren, J.; Lu, X.; Wang, M.; Peng, H. Winding Aligned Carbon Nanotube Composite Yarns into Coaxial Fiber Full Batteries with High Performances. *Nano Lett.* **2014**, *14*, 3432–3438.
11. Ren, J.; Zhang, Y.; Bai, W.; Chen, X.; Zhang, Z.; Fang, X.; Weng, W.; Wang, Y.; Peng, H. Elastic and Wearable Wire-Shaped Lithium-Ion Battery with High Electrochemical Performance. *Angew. Chem., Int. Ed.* **2014**, *53*, 7864–7869.
12. Zhong, J.; Zhang, Y.; Zhong, Q.; Hu, Q.; Hu, B.; Wang, Z. L.; Zhou, J. Fiber-Based Generator for Wearable Electronics and Mobile Medication. *ACS Nano* **2014**, *8*, 6273–6280.
13. Chu, Z.; Sarrob, P. M.; Middelhoeka, S. Silicon Three-Axial Tactile Sensor. *Sens. Actuators, A* **1996**, *54*, 505–510.
14. Wolenbuttel, M. R.; Regtien, P. P. L. Polysilicon Bridges for the Tealization of Tactile Sensors. *Sens. actuators, A* **1991**, *26*, 257–264.
15. Zhang, L. M.; Xue, F.; Du, W.; Han, C. B.; Zhang, C.; Wang, Z. L. Transparent Paper-Based Ttriboelectric Nanogenerator as Page Mark and Anti-Theft Sensor. *Nano Res.* **2014**, *7*, 1215–1223.
16. Wang, Z. L.; Song, J. H. Piezoelectric Nanogenerators Based on Zinc Oxide Nanowire Arrays. *Science* **2006**, *312*, 242–246.
17. Hansen, B. J.; Liu, Y.; Yang, R.; Wang, Z. L. Hybrid Nanogenerator for Concurrently Harvesting Biomechanical and Biochemical Energy. *ACS Nano* **2010**, *4*, 3647–3652.
18. Han, M.; Zhang, X. S.; Meng, B.; Liu, W.; Tang, W.; Sun, X. M.; Wang, W.; Zhang, H. X.R-Shaped Hybrid Nanogenerator with Enhanced Piezoelectricity. *ACS Nano* **2013**, *7*, 8554–8560.
19. Hu, Y.; Yang, J.; Niu, S.; Wu, W.; Wang, Z. L. Hybridizing Triboelectrification and Electromagnetic Induction Effects for High-Efficient Mechanical Energy Harvesting. *ACS Nano* **2014**, *8*, 7442–7450.
20. Lin, Z.-H.; Cheng, G.; Wu, W.; Pradel, C. K.; Wang, Z. L. Dual-Mode Triboelectric Nanogeneratorfor Harvesting Water Energy and as aSelf-Powered Ethanol Nanosensor. *ACS Nano* **2014**, *8*, 6440–6448.
21. Fan, F. R.; Tian, Z. Q.; Wang, Z. L. Flexible Triboelectric Generator. *Nano Energy* **2012**, *1*, 328–334.
22. Niu, S.; Wang, S.; Liu, Y.; Zhou, Y. S.; Lin, L.; Hu, Y.; Pradel, C. K.; Wang, Z. L. A Theoretical Study of Grating Structured Triboelectric Nanogenerators. *Energy Environ. Sci.* **2014**, *7*, 2339–2349.
23. Liao, Q.; Zhang, Z.; Zhang, X.; Mohr, M.; Zhang, Y.; Fecht, H. J. Flexible Piezoelectric Nanogenerators Based on Fiber/ZnO Nanowires/Paper Hybrid Structure for Energy Harvesting. *Nano Res.* **2014**, *7*, 917–928.
24. Liao, Q.; Mohr, M.; Zhang, X.; Zhang, Z.; Zhang, Y.; Fecht, H. J. Carbon Fiber−ZnO Nanowire Hybrid Structures for Flexible and Adaptable Strain Sensors. *Nanoscale* **2013**, *5*, 12350–12355.
25. Pradel, K. C.; Wu, W.; Zhou, Y.; Wen, X.; Ding, Y.; Wang, Z. L. Piezotronic Effect in Solution-Grown p-Type ZnO Nanowires and Films. *Nano Lett.* **2013**, *13*, 2647–2653.
26. Yang, R. S.; Qin, Y.; Dai, L. M.; Wang, Z. L. Power Generation with Laterally Packaged Piezoelectric Fine Wires. *Nat. Nanotechnol.* **2009**, *4*, 34–39.
27. Egusa, S.; Wang, Z.; Chocat, N.; Ruff, Z. M.; Stolyarov, A. M.; Shemuly, D.; Sorin, F.; Rakich, P. T.; Joannopoulos, J. D.; Fink, Y. Multimaterial Piezoelectric Fibres. *Nat. Mater.* **2010**, *9*, 643–648.
28. Wei, A.; Sun, X.; Xu, C.; Dong, Z. L.; Yu, M. B.; Huang, W. Stable Field Emission from Hydrothermally Grown ZnO Nanotubes. *Appl. Phys. Lett.* **2006**, 88.
29. Joo, J.; Chow, B. Y.; Prakash, M.; Boyden, E. S.; Jacobson, J. M. Face-Selective Electrostatic Control of Hydrothermal Zinc Oxide Nanowire Synthesis. *Nat. Mater.* **2011**, *10*, 596–601.
30. Li, C.; Li, C.; Di, Y.; Lei, W.; Chen, J.; Cui, Y. Electron Field Emitters on Three-Dimensional Patterned Carbon Nanotube Framework. *ACS Appl. Mater. Interfaces* **2013**, *5*, 9194–9198.